Bond Alternation and Unpaired Spin Distributions in the Radical Anions of Cyclooctatetraene and Monosubstituted Derivatives. An ab Initio Study

James H. Hammons,*,† David A. Hrovat,‡ and Weston Thatcher Borden‡

Contribution from the Department of Chemistry, Swarthmore College, Swarthmore, Pennsylvania 19081, and Department of Chemistry, University of Washington, Seattle, Washington 98195. *Received December 3, 1990*

Abstract: Ab initio UHF, ROHF, and CI calculations have been performed on the radical anion of 1,3,5,7-cyclooctatetraene ($COT^{\bullet-}$) with the 3-21G and 6-31G* basis sets. At the UHF level, a D_{4h} structure with alternating bond angles was spuriously found to be lower in energy than a D_{4h} structure with alternating bond lengths. However, CI calculations showed that the true energy minima on the potential surface for $COT^{\bullet-}$ pseudorotation are a pair of equivalent, bond-alternated D_{4h} structures, which are connected by a pair of angle-alternated D_{4h} transition states, lying 4-5 kcal/mol higher in energy. At this level of theory, the calculated hyperfine coupling constant in $COT^{\bullet-}$ is in excellent agreement with that measured by EPR. Calculations on methyl-, fluoro-, and cyano-$COT^{\bullet-}$ have also been performed, and the computed hyperfine coupling constants for these derivatives of $COT^{\bullet-}$ are reported. These three substituents are calculated to have little effect on the degree of bond alternation in $COT^{\bullet-}$, but fluoro and cyano are each found to reduce the barrier to bond equalization by more than 50%.

One of the first open-shell annulenes to be observed experimentally was the radical anion of cyclooctatetraene ($COT^{\bullet-}$). In 1960, Katz and Strauss reported that the EPR spectrum of $Li^+COT^{\bullet-}$ in THF showed eight equivalent hydrogens, with a hyperfine coupling constant of -3.209 G.[1] The resulting value of -25.67 G for Q, the constant in the McConnell equation, lies well within the range that is typical of planar annulene radicals and radical ions. The EPR spectra of 1,2-[2] and 1,4-dialkyl-$COT^{\bullet-}$[3] showed similar Q values and, like $COT^{\bullet-}$ itself, uniform distributions of unpaired spin. Evidence from NMR,[4] EPR line broadening,[5] UV-visible,[6] and polarographic[7] experiments also suggests that $COT^{\bullet-}$ is planar or nearly planar. Several theoretical treatments of $COT^{\bullet-}$ by semiempirical methods have indicated a bond-alternated (D_{4h}) equilibrium geometry, with the unpaired spin density evenly distributed over the ring.[8-10]

In contrast, most $COT^{\bullet-}$ derivatives that are monosubstituted or that bear substituents only at the odd-numbered ring carbons show pronounced alternations of unpaired spin between the odd- and even-numbered carbons around the $COT^{\bullet-}$ ring.[11-13] In pioneering theoretical papers, McLachlan and Snyder[8] and Moss[9] have discussed the role of configuration interaction, vibronic coupling, and Boltzmann mixing in determining the electronic structure of $COT^{\bullet-}$ and monosubstituted derivatives, but the power of modern computational methodology has not yet been brought to bear on this problem. In this paper, we report the results of ab initio UHF, ROHF, and CI calculations on the electronic and molecular structure of $COT^{\bullet-}$ and of its methyl, fluoro, and cyano derivatives.

Real and Artifactual Symmetry Breaking[14] in $COT^{\bullet-}$

Because three electrons occupy a pair of e_{2u} orbitals in D_{8h} $COT^{\bullet-}$, a first-order Jahn-Teller effect must occur.[8,9] Group theory shows that the Jahn-Teller-active vibrational modes of D_{8h} $COT^{\bullet-}$ belong to the b_{1g} and b_{2g} representations of the D_{8h} point group. Both modes yield structures of D_{4h} symmetry. However, upon a b_{1g} distortion from D_{8h} symmetry, larger and smaller bond angles alternate around the ring, and the C-C bond lengths remain equal. In contrast, for a b_{2g} distortion of the ring, the C-C-C bond angles all remain 135°, but shorter and longer C-C bond lengths alternate around the ring. These three geometries for the carbon skeleton are depicted in Figure 1.

The forms of the symmetry-correct, nonbonding (NB)MOs, which are illustrated in Figure 2, differ for the two different types of D_{4h} geometries. For an angle-alternated structure, the correct NBMOs are

$$\psi_4 = 0.50(\phi_1 - \phi_3 + \phi_5 - \phi_7)$$
$$\psi_5 = 0.50(\phi_2 - \phi_4 + \phi_6 - \phi_8) \quad (1)$$

With ψ_4 filled and ψ_5 half-filled, the negative charge in $COT^{\bullet-}$ would be concentrated on the four odd-numbered ring carbons and the unpaired π spin on the four even-numbered positions.

For a D_{4h} geometry in which the C-C bond lengths alternate, the appropriate NBMOs can be expressed as linear combinations of the NBMOs in eq 1.

$$\psi_4' = (\psi_4 + \psi_5)/2^{1/2} = 0.35(\phi_1 + \phi_2 - \phi_3 - \phi_4 + \phi_5 + \phi_6 - \phi_7 - \phi_8)$$
$$\psi_5' = (\psi_4 - \psi_5)/2^{1/2} = 0.35(\phi_1 - \phi_2 - \phi_3 + \phi_4 + \phi_5 - \phi_6 - \phi_7 + \phi_8) \quad (2)$$

In the NBMO that is preferentially occupied by two of the three electrons, the positive and negative overlaps between adjacent AOs occur, respectively, along the short and long C-C bonds. The other NBMO, in which the signs of the overlaps are reversed, is occupied by the unpaired electron. The resulting wave function spreads

† Visiting Professor at the University of Washington from Swarthmore College, 1989.
‡ University of Washington.

(1) Katz, T. J.; Strauss, H. L. *J. Chem. Phys.* **1960**, *32*, 1873-1875.
(2) (a) Blankespoor, R. L.; Snavely, C. M. *J. Org. Chem.* **1976**, *41*, 2071-2073. (b) Bauld, N. L.; Farr, F. R.; Hudson, C. E. *J. Am. Chem. Soc.* **1974**, *96*, 5634-5635.
(3) Hammons, J. H.; Kresge, C. T.; Paquette, L. A. *J. Am. Chem. Soc.* **1976**, *98*, 8172-8174.
(4) Katz, T. J. *J. Am. Chem. Soc.* **1960**, *82*, 3785-3786.
(5) Strauss, H. L.; Katz, T. J.; Fraenkel, G. K. *J. Am. Chem. Soc.* **1963**, *85*, 2360-2364.
(6) Kimmel, P. I.; Strauss, H. L. *J. Phys. Chem.* **1968**, *72*, 2813-2817.
(7) Allendoerfer, R. D.; Rieger, P. H. *J. Am. Chem. Soc.* **1965**, *87*, 2336-2344. For an opposing conclusion, however, see: Anderson, L. B.; Hansen, J. F.; Kakihana, T.; Paquette, L. A. *J. Am. Chem. Soc.* **1971**, *93*, 161-167.
(8) (a) McLachlan, A. D.; Snyder, L. C. *J. Chem. Phys.* **1962**, *36*, 1159-1162. (b) Snyder, L. C. *J. Phys. Chem.* **1964**, *66*, 2299-2306.
(9) Moss, R. E. *Mol. Phys.* **1966**, *10*, 501-516.
(10) Dewar, M. J. S.; Harget, A.; Haselbach, E. *J. Am. Chem. Soc.* **1969**, *91*, 7521-7523.
(11) See, for example: Carrington, A.; Todd, P. F. *Mol. Phys.* **1964**, *7*, 533-540.
(12) Stevenson, G. R.; Concepcion, J. G.; Echegoyen, L. *J. Am. Chem. Soc.* **1974**, *96*, 5452-5455.
(13) Hammons, J. H.; Bernstein, M.; Myers, R. J. *J. Phys. Chem.* **1979**, *83*, 2034-2040.
(14) Review: Davidson, E. R.; Borden, W. T. *J. Phys. Chem.* **1983**, *87*, 4783-4790.

0002-7863/91/1513-4500$02.50/0

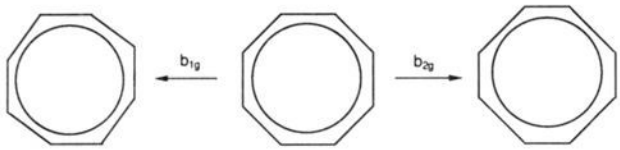

2 1 3

Figure 1. Schematic depiction of the effect of b_{1g} and b_{2g} distortions of D_{8h} $COT^{\bullet-}$, **1**, leading, respectively, to D_{4h} geometries **2** and **3**, with alternation of bond angles in **2** and bond lengths in **3**.

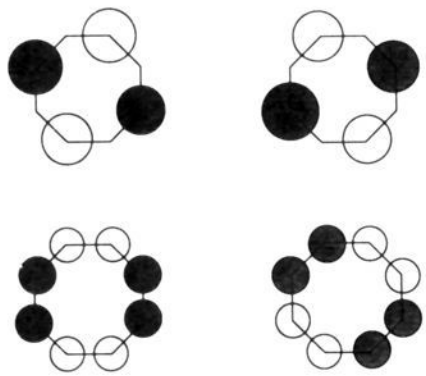

Figure 2. Schematic depiction of the NBMOs for D_{8h} $COT^{\bullet-}$: top, NBMOs appropriate for describing distortions to D_{4h} geometries with alternating bond angles; bottom, NBMOs appropriate for describing distortions to D_{4h} geometries with alternating bond lengths.

both the negative charge and the unpaired π-spin density uniformly over all eight ring carbons.

At D_{8h} geometries, both pairs of NBMOs belong to the e_{2u} representation, and either pair of MOs is symmetry-correct. Depending on the choice of coordinate axes, calculations on $COT^{\bullet-}$ in D_{8h} symmetry can be made to yield either set of orbitals. Since the energy of $COT^{\bullet-}$ cannot depend on the choice of coordinate axes, both sets of orbitals should give the same energy at D_{8h} geometries. However, this may not be the case for the energies calculated from approximate wave functions that utilize the two different sets of orbitals.[15]

For example, the set of NBMOs in eq 1 localizes the unpaired π electron to four, nonadjacent carbons. In a UHF wave function, this results in spin polarization of "paired" π electrons, so that electrons of opposite spin occupy spatially different MOs. Those electrons with the same spin as the unpaired electron tend to concentrate on the same four carbons as the unpaired electron, while those of opposite spin, which try to avoid the unpaired electron, tend to concentrate more on the remaining four carbons.

In contrast, the set of NBMOs in eq 2 provides a uniform distribution of both spin and charge. Thus, because of the uniform distribution of the unpaired π electron over the ring, there can be no spin polarization of the paired π electrons when these MOs are used. As a result, UHF calculations on D_{8h} $COT^{\bullet-}$ are expected to give a lower energy when the D_{4h} NBMOs in eq 1 are used than when the D_{4h} NBMOs in eq 2 are employed.[15] To the extent that this is actually found to be the case, UHF calculations on $COT^{\bullet-}$ are inadequate.

Although a geometry of D_{8h} symmetry cannot be the equilibrium geometry of $COT^{\bullet-}$, it is crucial that both sets of D_{4h} MOs give the same energies at D_{8h} geometries. Since one set of NBMOs is appropriate for describing b_{1g} bond angle distortions from D_{8h} geometries and the other is appropriate for b_{2g} bond length distortions, unless the two sets of D_{4h} MOs give the same energies at D_{8h} geometries, it is highly unlikely that the relative energies of the two types of D_{4h} distorted geometries will be calculated correctly. The accurate calculation of the relative energies of the two types of D_{4h} geometries is important because one set is expected to be the minima and the other the local maxima on the pathway for pseudorotation of $COT^{\bullet-}$ from one equivalent, D_{4h} geometry to another.[15]

(15) For a closely related example, see: Borden, W. T.; Davidson, E. R.; Feller, D. *J. Am. Chem. Soc.* **1981**, *103*, 5725–5729.

Table I. Optimized Bond Distances (Å) and Angles (deg) for Several Geometries of $COT^{\bullet-}$, Calculated at the UHF/3-21G Level of Theory

geometry	CC distances	CH distances	CCC angles	CCH angles
D_{8h}	1.399[a]	1.080	135.0	112.5
D_{4h}, angle	1.399	1.083, 1.080	136.6, 133.4	111.7, 113.3
D_{4h}, bond	1.359, 1.435	1.081	135.0	113.4[b]

[a] Optimized with the NBMOs in eq 1. Using the NBMOs in eq 2 gives an optimized C–C bond distance of 1.394 Å. [b] C=C—H angle.

Table II. Relative Energies (kcal/mol) for Various Geometries of $COT^{\bullet-}$, Calculated with the 3-21G Basis Set

geometry	NBMOs	UHF	ROHF	π-SD CI	π-SD + σ-S CI	π-SD, σ-S CI
D_{4h}, bond	eq 2	0[a]	0[b]	0[c]	0[d]	0[e]
D_{4h}, angle	eq 1	−7.4	4.1	2.5	3.2	3.8
D_{8h}	eq 2	5.5	5.9	3.9	3.2	4.0
D_{8h}	eq 1	−6.8	4.8	3.0	3.7	4.3

[a] Energy relative to −305.7695 hartrees. [b] Energy relative to −305.7663 hartrees. [c] Energy relative to −305.8665 hartrees. [d] Energy relative to −305.8865 hartrees. [e] Energy relative to −306.0774 hartrees.

In order to obtain reliable relative energies for the two types of optimized D_{4h} geometries, it is necessary to perform calculations at a level of theory that is sufficient to give the same energies for D_{8h} geometries, starting with either set of D_{4h} MOs. Previous computational studies of other open-shell molecules that are charged[14-16] or that contain charge separation[17] indicated that multiconfiguration calculations, which included $\sigma-\pi$ as well as $\pi-\pi$ correlation, would be required.

Computational Methodology

Geometries were optimized with UHF calculations, performed with the 3-21G basis set.[18] Optimizations were carried out for D_{8h} and for bond- and angle-alternated D_{4h} geometries. In order to ensure that basis set expansion had a negligible effect on the geometries obtained, selected geometries were reoptimized with the 6-31G* basis set.[19] Attempts to perform UHF calculations with additional diffuse functions included in the basis set were foiled by convergence problems. Vibrational analyses were performed at the UHF/3-21G level to determine whether each stationary point was a minimum or an energy maximum in one or more normal coordinates. All of the UHF calculations were carried out with use of the Gaussian 86 package of programs.[20] The optimized geometries are presented in Table I.

The effect of electron correlation on the relative energies of $COT^{\bullet-}$ at the UHF-optimized geometries was investigated by CI calculations, carried out with the MELDF package of programs.[21] Starting with ROHF wave functions, three different types of CI calculations were performed at each geometry—all single and double excitations among the π MOs (π-SD CI), π-SD CI plus all single excitations among the σ MOs (π-SD + σ-S CI), and π-SD and σ-S CI, with π-S and σ-S excitations allowed simultaneously (π-SD, σ-S CI). The UHF, ROHF, and CI energies obtained are summarized in Table II.

For a monosubstituted $COT^{\bullet-}$, an angle-alternated geometry has C_{2v} symmetry, but a bond-alternated geometry can have at most the plane of the eight-membered ring as a symmetry element. Thus, unlike the case

(16) Hrovat, D. A.; Borden, W. T. *J. Am. Chem. Soc.* **1985**, *107*, 8034–8035. Du, P.; Borden, W. T. *J. Am. Chem. Soc.* **1987**, *109*, 5330–5336. Du, P.; Hrovat, D. A.; Borden, W. T. *J. Am. Chem. Soc.* **1988**, *110*, 3405–3412.

(17) Du, P.; Hrovat, D. A.; Borden, W. T. *J. Am. Chem. Soc.* **1989**, *111*, 3773–3778. Coolidge, M. B.; Yamashita, K.; Morokuma, K.; Borden, W. T. *J. Am. Chem. Soc.* **1990**, *112*, 1751–1754.

(18) Binkley, J. S.; Pople, J. A.; Hehre, W. J. *J. Am. Chem. Soc.* **1980**, *102*, 939–947.

(19) Hariharan, P. C.; Pople, J. A. *Theor. Chim. Acta* **1973**, *28*, 213–222.

(20) Frisch, M.; Binkley, J. S.; Schlegel, H. B.; Raghavachari, K.; Martin, R.; Stewart, J. J. P.; Bobrowicz, F.; Defrees, D.; Seeger, R.; Whiteside, R.; Fox, D.; Fluder, E.; Pople, J. A. Carnegie-Mellon University.

(21) Developed at the University of Washington by McMurchie, L.; Elbert, S.; Langhoff, S.; and Davidson, E. R. and modified by Feller, D. and Rawlings, D.

Table III. Relative π-SD + σ-S CI/3-21G Energies (kcal/mol) for Various Geometries of $COT^{\bullet-}$ and of Fluoro, Methyl, and Cyano Derivatives

substituent	bond-alternated	midpoint	angle-alternated	minimum[a]
H	0[b]	0.3	3.2	−1.4
F[c]	0[d]	−0.3	0.7	−0.7
F[e]	0[f]	0.1	1.1	−0.5
CH_3	0[g]	0.4	3.0	−1.2
CN	0[h]	0.0	1.3	−0.7

[a] Obtained by fitting the energies calculated at the first three geometries, as described in the text. [b] Energy relative to −305.8865 hartrees. [c] Ring geometries assumed. [d] Energy relative to −404.2350 hartrees. [e] Bond-alternated and angle-alternated geometries optimized at the ROHF level. [f] Energy relative to −404.2360 hartrees. [g] Energy relative to −344.7132 hartrees. [h] Energy relative to −397.1593 hartrees.

in the parent radical anion, where symmetry constraints can be used to allow the optimization of a bond-alternated geometry, this is not possible in monosubstituted derivatives of $COT^{\bullet-}$. The finding (Table II) that, as expected (vide supra), UHF calculations spuriously favor angle-alternated ring geometries for $COT^{\bullet-}$, thus, made it impossible for us to perform UHF calculations in order to optimize bond-alternated ring geometries for monosubstituted derivatives of $COT^{\bullet-}$.

Ring geometries for methyl-, fluoro-, and cyano-substituted $COT^{\bullet-}$ were obtained from the UHF-optimized ring geometries for the parent $COT^{\bullet-}$. In addition to the angle- and bond-alternated ring geometries, a third geometry, having both bond angles and bond lengths exactly halfway between the angle- and bond-alternated extremes (i.e., a C_{4h} geometry for the ring carbons), was used. The bond lengths and bond angles for the fluoro and cyano substituents were optimized at the UHF/3-21G level, with the ring frozen at the bond-angle-alternated D_{4h} geometry found for $COT^{\bullet-}$. These parameters for the fluoro and cyano substituents were then used for calculations at all three ring geometries. The local geometry of the methyl substituent was optimized separately for each of the three ring geometries. The π-SD + σ-S CI energies for these three $COT^{\bullet-}$ derivatives at each of the three geometries are given in Table III.

As a check on the accuracy of using assumed ring geometries for these monosubstituted derivatives of $COT^{\bullet-}$, the geometry of the fluoro-substituted anion was optimized at the ROHF level of theory, both in C_{2v} and in C_s symmetries. A third, "midpoint" geometry for CI calculations was obtained by interpolating between the optimized angle-alternated and bond-alternated geometries. These three geometries are available as supplementary material.[22] The ROHF energy at each of these three "optimized" geometries was slightly less than 2 kcal/mol lower than the ROHF energy at the corresponding assumed ring geometry. The π-SD + σ-S CI energies computed at the ROHF-optimized geometries are given in Table III.

Results and Discussion

Optimized Geometries. As shown in Table I, the bond lengths in the optimized D_{8h} and angle-alternated D_{4h} structures for $COT^{\bullet-}$ are very similar and the bond angles in the latter differ from the regular octagonal values by just 1.6°. The alternation of C–C distances in the bond-alternated geometry, while appreciably less than is found in the neutral molecule,[23] is substantial; the short and long C–C bonds differ in length by 0.076 Å. Previous geometry optimizations of this structure by modified Hückel[8b] and MINDO/2[10] methods have given longer C–C bond lengths and slightly less bond alternation.

UHF reoptimization of the bond-alternated D_{4h} structures with the 6-31G* basis set gave R(C—C) = 1.363 and 1.438 Å, R(C—H) = 1.083 Å, C—C—C = 135.0°, and C=C—H = 113.2°. These values are nearly the same as those obtained with 3-21G.

Although UHF/3-21G vibrational analyses found real frequencies for all of the out-of-plane vibrations at both types of optimized D_{4h} geometries for $COT^{\bullet-}$, we were anxious to confirm that a planar geometry was also an energy minimum at the UHF/6-31G* level. Unfortunately, attempts to perform a UHF/6-31G* vibrational analysis on the optimized, bond-alternated, D_{4h} geometry were unsuccessful, because the storage requirements exceeded the available memory. Therefore, attempts were made with the 6-31G* basis set to optimize a nonplanar, bond-length-alternated, D_{2d} structure. However, the optimization converged back to the D_{4h} structure. Thus, in contrast to the D_{2d} equilibrium geometry of neutral COT,[23] our calculations give no indication of a nonplanar equilibrium geometry for $COT^{\bullet-}$.

Energies. As shown in Table II, at the UHF level of theory, the energy of the angle-alternated D_{4h} structure is 7.4 kcal/mol lower than that of the D_{4h} structure with alternating bond lengths. Physically, this result is surprising, because one might have imagined that distortion of the bond lengths in $COT^{\bullet-}$ from D_{8h} symmetry would have provided a greater energy lowering than distortion of the bond angles. In fact, the data in Table II actually show this to be the case, when the energy differences are taken between comparable D_{8h} and D_{4h} calculations.

Since the NBMOs in eq 2 must be used for calculations at D_{4h} geometries with alternating C–C bond lengths, the energy of this type of optimized D_{4h} geometry should be compared with the energy of the D_{8h} geometry that is calculated with the same set of MOs. Similarly, since the NBMOs in eq 1 must be used for calculations at D_{4h} geometries with alternating bond angles, the energy of this type of optimized D_{4h} geometry too should be compared with the energy of the D_{8h} geometry that is calculated with the same set of MOs. These comparisons show that distortion of the bond lengths in $COT^{\bullet-}$ from D_{8h} symmetry lower the UHF energy by 5.5 kcal/mol, whereas bond angle distortions result in an energy lowering of only 0.6 kcal/mol.

The UHF energy of the D_{4h} geometry with alternating bond angles is, nevertheless, lower than that of the D_{4h} geometry with alternating bond lengths, because, as anticipated, the NBMOs of eq 1 provide more π-electron correlation at the UHF level than do the NBMOs of eq 2.[24] This is shown clearly by the UHF energy, computed at the optimized D_{8h} geometry, which is 12.3 kcal/mol lower when the NBMOs of eq 1 are used than when the NBMOs of eq 2 are employed. The fact that such different UHF energies are obtained at the same D_{8h} geometry, depending on the totally arbitrary choice of which set of NBMOs is used, is prima facie evidence that UHF calculations do not provide a satisfactory description of $COT^{\bullet-}$.

The ROHF calculations, which restrict the paired electrons to spatially identical orbitals, do not allow spin polarization. Consequently, ROHF calculations avoid the large difference in the amount of π-electron correlation that exists between the two UHF wave functions constructed from the two different sets of NBMOs. Nevertheless, the ROHF energies for the D_{8h} structure still differ, because the NBMOs in eq 2 give a smooth distribution of negative charge, whereas those in eq 1 give an uneven distribution of π charge. The latter set of NBMOs thus allow for some correlation between one of the nonbonding electrons and the bonding electrons. This correlation is not contained in ROHF wave functions that are constructed from the former set of NBMOs.[15] However, the energy difference between the two types of ROHF wave functions at the D_{8h} geometry amounts to only 1.1 kcal/mol. This discrepancy is small enough to allow ROHF calculations to predict correctly that the energy minimum is the bond-alternated D_{4h} structure, which is computed to be 4.1 kcal/mol below the angle-alternated D_{4h} geometry.

All three levels of CI calculations also find the bond-alternated D_{4h} structure to lie below the angle–alternated D_{4h} geometry. As expected, the π-SD CI calculations, which do not explicitly include σ–π-electron correlation, give the poorest results. The two π-SD CI wave functions for the D_{8h} geometry differ in energy by 0.9

(22) Ordering information is given on any current masthead page.

(23) Bastiansen, O.; Hedberg, L.; Hedberg, K. *J. Chem. Phys.* **1957**, *27*, 1311.

(24) Despite the lower UHF energy of the angle-alternated geometry, the UHF vibrational analysis at the bond-alternated geometry did not show a negative force constant for a vibration that caused the bond angles to alternate in size. This result is due to the fact that second derivatives of the wave function were obtained analytically, rather than by finite differences. Had finite differences been used, calculations at angle-alternated geometries would have allowed the UHF wave function to break symmetry, leading to different spin densities on the two different sets of carbons and to a discontinuous lowering of the UHF energy.[14-16]

kcal/mol, which is only slightly smaller than the difference found at the ROHF level. Polarization of the σ electrons by the uneven distribution of π charge that is provided by the NBMOs in eq 1 furnishes a type of correlation between σ and π electrons that is not available when the NBMOs of eq 2 are used.

The remaining two sets of CI calculations both include single excitations of σ electrons. The first type of calculation, which includes about 3300 spin-adapted configurations, allows the σ electrons to correlate with only the frozen ROHF portion of the π wave function. This amount of σ-π correlation reduces the energy difference between the two D_{8h} calculations to only 0.4 kcal/mol. The second type of calculation includes much more extensive σ-π correlation by allowing simultaneous excitation of one electron of each kind from the MO it occupies in the ROHF wave function. These π-SD,σ-S CI calculations each contain over 49 000 spin-adapted configurations, and reduce the energy difference between the two wave functions to just 0.3 kcal/mol. At this level of CI, the energy difference between the pair of equivalent, bond-length-alternated, D_{4h} minima on the $COT^{\bullet-}$ potential surface and the pair of equivalent, angle-alternated, D_{4h} transition states that connect them amounts to 3.8 kcal/mol.

Monosubstituted Derivatives of $COT^{\bullet-}$. The introduction of a single substituent on the D_{8h} $COT^{\bullet-}$ ring removes the degeneracy of the NBMOs in eq 1.[25] If the substituent at C-1 is a π-electron donor like fluorine, the NBMO in eq 1 that has density at C-1 will be destabilized and will be occupied by only one of the three nonbonding electrons. The other two electrons will preferentially occupy the remaining NBMO, which has a node at C-1. In contrast, if the substituent is a π acceptor, like cyano, the electron pair will preferentially occupy the NBMO that has density at C-1 and the unpaired electron will be relegated to the NBMO that has a node at this carbon.

In the parent $COT^{\bullet-}$, mixing between the NBMOs in eq 1, induced by a distortion to a bond-alternated geometry, results in a first-order Jahn–Teller effect. Because the NBMOs in eq 1 are degenerate in the parent D_{8h} $COT^{\bullet-}$, they are mixed equally by such a distortion. Therefore, the resulting MOs (eq 2) have equal coefficients at each carbon.

In contrast, in a monosubstituted derivative of $COT^{\bullet-}$, the orbitals in eq 1 no longer have the same energy, and so they are not equally mixed by such a molecular distortion, which is now termed a second-order Jahn–Teller effect.[14] Consequently, unlike the orbitals (eq 2) for the bond-alternated geometries of the parent $COT^{\bullet-}$, the orbitals for bond-alternated geometries of a monosubstituted derivative will not have equal coefficients at each carbon. Thus, bond alternation is not expected to provide as much energy lowering in monosubstituted derivatives of $COT^{\bullet-}$ as in the parent radical anion. Since either a π-donor or a π-acceptor substituent can lift the degeneracy of the NBMOs that are mixed by bond alternation, the amount of stabilization provided by bond alternation is anticipated to decrease as the π-electron-donating or -accepting ability of the substituent increases.

As in the parent $COT^{\bullet-}$, UHF calculations on monosubstituted derivatives are not expected to give reliable results for the relative energies of bond- and angle-alternated geometries. We would have liked to perform π-SD,σ-S CI calculations on the monosubstituted derivatives of $COT^{\bullet-}$, but their low symmetry (only C_s at bond-alternated geometries, compared to D_{4h} in the parent) made such calculations prohibitively large. However, we were able to perform CI calculations at the π-SD + σ-S level.

Table III presents the relative π-SD + σ-S CI energies obtained at the bond- and angle-alternated ring geometries for $COT^{\bullet-}$ and for fluoro-, methyl-, and cyano-$COT^{\bullet-}$. Also given for these COT radical anions is the CI energy at a ring geometry that is at the midpoint between the two extremes of only bond length and only bond angle alternation.

By fitting the π-SD + σ-S CI energies at these three geometries for each radical anion with a potential function that contained quadratic and quartic terms in the difference between the two sets of C–C bond lengths, we obtained a rough estimate of the extent of bond alternation at the minimum energy ring geometry and the relative energy at this geometry. For the parent $COT^{\bullet-}$, the fit to the CI energies yielded a difference of 0.061 Å between the long and short bonds, compared to 0.076 Å at the UHF level. As shown in Table III, the interpolated CI energy at the CI minimum is 1.4 kcal/mol below the CI energy at the UHF bond-alternated geometry.[26]

For the substituted radical anions, the estimated alternation in the C–C bond lengths at the minimum energy geometry of each is also about 0.06 Å.[27] The interpolated energies at the minima are given in Table III. The table shows that, at least for a fluoro substituent, full ROHF optimization of the ring geometries results in only a small change in the location or depth of the CI energy minimum.

The barrier height to bond equalization in each radical anion is just the energy difference between the geometry with only the bond angles alternated and the CI energy minimum. Listed by substituent, the barrier heights (kcal/mol) are as follows: R = H, 4.6; R = F, 1.4 (1.6); R = CH_3, 4.2; and R = CN, 2.0.

Our results support the qualitative expectation that strongly perturbing substituents on the $COT^{\bullet-}$ ring, such as F and CN, tend to lower significantly, on a percentage basis, the barrier to bond length equalization. Interestingly, it would appear that, although such substituents do tend to reduce this barrier, they have a much less dramatic effect on the extent of bond alternation. The effects of substituents on the distribution of unpaired spin in $COT^{\bullet-}$ is discussed in the next section.

Proton Hyperfine Coupling. Katz and Strauss[1] reported in 1960 that the EPR spectrum of $Li^+COT^{\bullet-}$ in THF consisted of nine equally spaced lines with the intensity ratios expected from hyperfine coupling to eight equivalent hydrogens. The proton hyperfine coupling constant measured under these conditions was −3.209 G. Essentially the same value has been obtained by subsequent measurements.[11]

Calculations on radicals with unpaired π electrons do not yield unpaired spin densities in σ orbitals, unless electron correlation is included at a level that allows an unpaired spin in a π orbital to polarize the σ electrons. Consequently, ROHF and π-SD CI calculations on $COT^{\bullet-}$ predict no proton hyperfine coupling, but UHF calculations and CI calculations that include σ-S excitations do give unpaired spin densities in the hydrogen 1s AOs. The unpaired spin densities can be multiplied by the hyperfine coupling constant in the hydrogen atom (509.74 gauss)[28] to obtain calculated values of the coupling constants (a_H) in $COT^{\bullet-}$.

For $COT^{\bullet-}$ at the UHF-optimized, D_{4h} geometry with alternating bond lengths, the calculated values of a_H in gauss at various levels are as follows: UHF/3-21G, −7.55; UHF/6-31G*, −7.90; π-SD + σ-S CI/3-21G, −4.03; and π-SD,σ-S CI/3-21G, −3.21. The magnitudes of a_H calculated at the UHF level are both more than 130% too large, while the magnitude of the value obtained with the lower level of σ-CI is too large by about 25%. However, the value of a_H calculated at the π-SD,σ-S level of CI is in essentially exact agreement with experiment.

Hyperfine coupling constants for many derivatives of $COT^{\bullet-}$ have also been reported.[11-13] Those that are monosubstituted or substituted only at the odd-numbered carbons show alternations of large and small hydrogen coupling constants around the eight-membered ring.[29] Substituents, like F, that are π-electron

(25) Since the molecular symmetry is reduced to C_{2v}, only the coefficients at atoms that remain symmetry-equivalent necessarily remain exactly equal in these MOs.

(26) π-SD,σ-S calculations gave essentially the same results. The minimum was found to occur at a difference of 0.062 Å between the lengths of the two types of ring bonds at an energy of −1.2 kcal/mol, relative to the UHF-optimized, bond-alternated minimum, giving a barrier to bond equalization of 5.0 kcal/mol.

(27) Although in each case the energies of the midpoint and bond-alternated geometries are very similar, the minimum energy geometry lies closer to the latter, because the term in the potential energy that favors bond alternation is quadratic in the deviation from equality, whereas the term that favors a geometry with equal C–C bond lengths is quartic.

(28) Wertz, J. E.; Bolton, J. R. *Electron Spin Resonance: Elementary Theory and Practical Applications*; McGraw-Hill, Inc.: New York, 1972; p 443.

Table IV. Comparison of the Experimental Hyperfine Coupling Constants (G) for the Ring Protons of Fluoro-, Methyl-, and Cyano-COT$^{\bullet-}$ with Those Calculated from the π-SD + σ-S Cl/3-21G Spin Populations at Bond-Alternated, Angle-Alternated, and Midpoint Geometries

substituent	position[a]	bond-alternated	midpoint	angle-alternated	experiment
F[b]	2, 8	−2.6	−1.2	0.8	0.16[c,d]
	3, 7	−5.3	−6.7	−8.6	−6.50
	4, 6	−2.5	−1.1	0.9	0.33[d]
	5	−5.3	−6.7	−9.1	−6.50
CH_3	2, 8	−3.3	−2.4	0.7	−1.40[c,e]
	3, 7	−4.5	−5.4	−8.4	−5.06
	4, 6	−3.3	−2.4	0.6	−1.40
	5	−4.6	−5.4	−8.4	−5.06
CN	2, 8	−4.9	−6.0	−6.9	−6.69[c]
	3, 7	−2.3	−1.0	0.9	0.53
	4, 6	−5.2	−6.6	−9.7	−7.52
	5	−1.9	−0.8	1.2	0.87

[a] For positions that are interchanged by rapid interconversion of the two equivalent, bond-length-alternated geometries, the calculated coupling constants have been averaged. [b] Obtained from calculations at assumed ring geometries. [c] Reference 13. [d] The signs of coupling constants with very small magnitudes are uncertain. [e] Reference 11.

donors tend to give large, negative coupling constants for the hydrogens attached to the odd-numbered ring carbons, while π acceptors, like CN, tend to give large, negative coupling constants for the hydrogens attached to even-numbered ring carbons.

The hyperfine coupling constants measured for F-, CH_3-, and CN-substituted COT$^{\bullet-}$ are given in Table IV. Also given are the calculated values, which were computed from the hydrogen 1s spin densities that were obtained from the π-SD + σ-S CI calculations on these derivatives of COT$^{\bullet-}$. The coupling constants were computed at each of the three different geometries, discussed in the previous section.[30]

Because a π-SD,σ-S CI calculation gives a value for a_H in the parent COT$^{\bullet-}$ that is in essentially perfect agreement with experiment, we would, of course, have preferred to perform calculations at this level for the F, CH_3, and CN derivatives. However, as noted in the previous section, CI calculations at this level on monosubstituted derivatives of COT$^{\bullet-}$ are too large to be practical.

The calculated coupling constants in Table IV are qualitatively similar to the experimental values in several respects, including the alternation of magnitude around the ring, as well as the larger size at the odd-numbered carbons in F–COT$^{\bullet-}$ and CH_3–COT$^{\bullet-}$ and at the even-numbered carbons in CN–COT$^{\bullet-}$. For F and CH_3 substituents, the calculated coupling constants show the same near equality of $a_{3,7}$ with a_5 and of $a_{2,8}$ with $a_{4,6}$ that is observed experimentally. Also in agreement with experiment, the calculated values of $a_{3,7}$ and a_5 differ in CN–COT$^{\bullet-}$, as do those of $a_{2,8}$ and $a_{4,6}$. The larger magnitude of the hyperfine coupling constant that is calculated at all geometries for the protons at C-2 and C-8 in CN–COT$^{\bullet-}$ provides a basis for assigning which pair of protons is responsible for the larger of the two-proton splittings that is observed experimentally.

The calculated coupling constants are geometry-dependent, because, as discussed in the previous section, the degree to which the unpaired electron is localized in one of the NBMOs of eq 1 depends on the degree to which bond alternation mixes these two NBMOs. For the C_{2v}, angle-alternated geometries, which have no bond length alternation, the unpaired π electron appears only at C-1,3,5 and 7 in F–COT$^{\bullet-}$ and in CH_3–COT$^{\bullet-}$ and at C-2,4,6, and 8 in CN–COT$^{\bullet-}$. The positive π-spin density at these carbons produces negative spin density in the 1s AOs of the hydrogens attached to them, which accounts for the large, negative coupling constants at the expected hydrogens in the angle-alternated geometry of each of these radical anions. The small, positive coupling constants for the remaining hydrogens are due to small, negative π-spin densities at the carbons where the singly occupied NBMO has nodes.

Bond alternation mixes the two NBMOs in eq 1, so that the resulting MO that is doubly occupied acquires π-bonding character along the shorter C–C bonds. With increasing alternation of the C–C bond lengths, the mixing of the two NBMOs changes the distribution of unpaired π spin from completely alternating to more nearly uniform. This change in π-spin distribution accounts for the changes in the calculated hyperfine coupling constants from alternating positive and negative to all negative as bond alternation increases.

The change in the π-spin distribution and, hence, in the hyperfine coupling constants with bond alternation is less for strongly perturbing substituents, like fluoro and cyano, than for methyl. A strongly perturbing substituent, whether a π donor, like fluoro, or a π acceptor, like cyano, creates a relatively large energy difference between the NBMOs in eq 1 at geometries with equal bond lengths. Thus, a fixed amount of bond length alternation provides less mixing of these MOs than when a more weakly perturbing substituent, like methyl, is present. This fact is responsible for both the lower stabilization on bond length alternation and for the less uniform hyperfine coupling constants at bond-alternated geometries that are calculated for fluoro and cyano substituents, compared to those for methyl.

Although the calculated hyperfine coupling constants in Table IV are in qualitative agreement with those found experimentally, it should be recalled that the CI energy minima for all three COT$^{\bullet-}$ derivatives are predicted to occur at ring geometries between the midpoint and the bond-alternated extreme and closer to the latter than to the former. However, if the observed coupling constants for each COT$^{\bullet-}$ derivative are compared with the calculated ones, the comparison in each case suggests a ring geometry that has even less bond length alternation than the midpoint geometry.

The quantitative discrepancy between the amount of bond alternation predicted at the CI equilibrium geometries of these derivatives of COT$^{\bullet-}$ and that indicated by comparison of the calculated and observed hyperfine coupling constants could have several possible sources. For example, a likely source of computational error is the computed hyperfine coupling constants, since π-SD + σ-S CI calculations on the parent COT$^{\bullet-}$ give coupling constants that are about 25% too large in magnitude. However, if the error in the π-SD + σ-S CI coupling constants for the COT$^{\bullet-}$ derivatives were in the same direction, even less bond length alternation would be indicated by comparison of a more accurate set of calculated hyperfine coupling constants with those that have been measured in these COT$^{\bullet-}$ derivatives.

Another possible source of computational error is the fact that assumed ring geometries have been used for calculations on these COT$^{\bullet-}$ derivatives. However, comparison of the results obtained for F–COT$^{\bullet-}$ at assumed and ROHF-optimized ring geometries shows ROHF geometry optimization to have little effect on the relative energies of the angle-alternated, midpoint, and bond-alternated species or on the calculated hyperfine coupling constants.[30] Nevertheless, since the potential surfaces for bond alternation in these COT$^{\bullet-}$ derivatives are obviously quite flat, it is conceivable that full geometry optimization at the CI level with a larger basis set would give equilibrium geometries that had less bond length alternation.

Precisely because our calculations predict that passage through geometries with equal bond lengths requires very little energy in COT$^{\bullet-}$ and derivatives, it is likely that vibrational excursions from the equilibrium geometries of these radical anions lead to very large contributions to the observed hyperfine coupling constants from geometries with ring bonds that are much more nearly equal in length than the ring bonds at the equilibrium geometry. This is especially likely to be the case in F–COT$^{\bullet-}$, where the barrier to bond equalization is calculated to be only 1.4 kcal/mol (1.6 kcal/mol with use of ROHF-optimized geometries), and in CN–COT$^{\bullet-}$, where the barrier is computed to be 2.0 kcal mol. Thus,

(29) Alternation of coupling constants can apparently also be induced by the metal counterions in a crystal containing COT$^{\bullet-}$: Jones, M. T.; de Boer, E. *Mol. Phys.* **1982**, *47*, 487–499.

(30) The ROHF-optimized and assumed geometries for angle-alternated F–COT$^{\bullet-}$ gave the same hyperfine coupling constants, and the ROHF-optimized and assumed ring geometries for the bond-alternated and midpoint structures gave hyperfine coupling constants that differed by only about 10%.

the hyperfine coupling constants measured in derivatives of $COT^{\bullet-}$ may be providing less information about the degree of bond alternation at the equilibrium geometries of these radical ions than about the ease with which geometries with more nearly equal bond lengths are accessed.

On the basis of INDO calculations, Hammons, Bernstein, and Myers[13] have advanced explanations of the effects of substituents on the EPR spectra of $COT^{\bullet-}$ that are similar to those presented here. Other researchers[12,31] have proposed an alternative model, which assumes bond alternation does not occur, so that the NBMOs in eq 1 are not mixed. Instead, this latter model postulates that there is a Boltzmann population of the lowest excited electronic state in which one electron is thermally excited from the lower energy of the two NBMOs to the upper.

Our CI calculations indicate that the basic assumption of the latter model is incorrect, since we find that bond alternation is energetically favorable, not only in $COT^{\bullet-}$, but also in its fluoro, methyl, and cyano derivatives. Our calculations suggest that these substituents have a relatively small effect on the extent of bond length alternation at the equilibrium geometry. However, both F, a π donor, and CN, a π acceptor, are found to reduce substantially the barrier to bond equalization.

Acknowledgment. We thank the National Science Foundation for its support of this research and for providing funds that enabled the purchase of the Convex C-2 computer, on which some of the calculations reported here were performed. We also thank the San Diego Supercomputer Center for a generous allocation of time on the Cray YMP-8/864 computer at SDSC.

Registry No. COT^-, 34510-85-5; F-COT^-, 70741-95-6; CH_3-COT^-, 34519-36-3; CN-COT^-, 70741-98-9.

Supplementary Material Available: ROHF/3-21G-optimized geometries and ROHF and CI energies for bond-alternated (C_s), angle-alternated (C_{2v}), and midpoint geometries of fluorocyclooctatetraene radical anion (2 pages). Ordering information is given on any current masthead page.

(31) Concepcion, J. G.; Vincow, G. *J. Phys. Chem.* **1975**, *79*, 2042-2048.

Molecular Mechanics (MM3) Calculations on Aldehydes and Ketones

Norman L. Allinger,* Kuohsiang Chen, Mita Rahman,[1] and Ahammadunny Pathiaseril[2]

Contribution from the School of Chemical Sciences, Department of Chemistry, University of Georgia, Athens, Georgia 30602. *Received July 26, 1990*

Abstract: Aldehydes and ketones have been studied in some detail by using the MM3 molecular mechanics method. Approximately 50 structures have been calculated and compared with experimental data where available. Comparisons are also made of conformational equilibria, torsional potentials, moments of inertia, vibrational spectra, heats of formation, and other data. On the whole, the calculations yield information of experimental accuracy. The exception is in the case of vibrational spectra, where the rms error over four simple compounds amounts to 42 cm^{-1}. Heats of formation for 35 compounds are calculated to within 0.41 kcal/mol.

Introduction

Earlier papers have described the MM3 force field,[3] which has previously been used for calculations on hydrocarbons,[4] alcohols and ethers,[5] amines,[6] alkenes,[7] and conjugated hydrocarbons.[8] The present work is concerned with the extension of these calculations to the important class of carbonyl compounds.

A comprehensive study of carbonyl compounds with an early force field was reported some years ago.[9,10] It was shown that in general, a great many structural features for these compounds could be well reproduced. At the time that work was carried out, the rotational profile about the central bond in 2-butanone was not known, and it was assumed to be quite similar to the similar profile in propanal. It was subsequently shown by ab initio calculations reported by Wiberg and Martin[11] that the gauche conformation is not really a stable conformation, separated by a significant barrier from the anti, but rather the gauche conformation is just a shoulder on the side of the anti potential well. This was corrected in MM2(77).[12,13]

Over the years it was shown[14] that there are many errors, mostly small, built into the MM2 force field. Rather than try to continue to patch these, it was decided to start again from the beginning and generate a new force field, which is called MM3. In addition to fitting the information which was previously fit for carbonyl compounds with MM2, including the corrected 2-butanone ro-

(1) Current address: Molecular Design Limited, 2132 Farallon Drive, San Leandro, CA 94577.

(2) This paper is taken in part from the Ph.D. Dissertation of A.P., submitted to the University of Georgia, March 1987. Current address: School of Pharmacy, Division of Medicinal Chemistry, 425 North Charter Street, University of Wisconsin, Madison, WI 53706.

(3) The MM3 program is available from the Technical Utilization Corporation, Incorporated, 235 Glen Village Court, Powell, OH 43065, and from Molecular Design Limited, 2132 Farallon Drive, San Leandro, CA 94577. The current version is available to run on VAX computers. Modifications for other machines are being made, and interested parties should contact one of the distributors directly.

(4) Allinger, N. L.; Yuh, Y. H.; Lii, J.-H. *J. Am. Chem. Soc.* **1989**, *111*, 8551, 8566, 8576.

(5) Allinger, N. L.; Rahman, M.; Lii, J.-H. *J. Am. Chem. Soc.* **1990**, *112*, 8293.

(6) Schmitz, L. R.; Allinger, N. L. *J. Am. Chem. Soc.* **1990**, *112*, 8307.

(7) Allinger, N. L.; Li, F.; Yan, L. *J. Comput. Chem.* **1990**, *11*, 848.

(8) Allinger, N. L.; Li, F.; Yan, L.; Tai, J. C. *J. Comput. Chem.* **1990**, *11*, 868.

(9) Allinger, N. L.; Tribble, M. T., Miller, M. A. *Tetrahedron* **1972**, *28*, 1173-1190.

(10) Profeta, S., Jr.; Allinger, N. L., this work was never published in the ordinary way, but the results of it were included in the MM2 parameter set (ref 15). An updated modification of this work was published in ref 12.

(11) Wiberg, K. B.; Martin, E. *J. Am. Chem. Soc.* **1985**, *107*, 5035.

(12) Bowen, P.; Pathiaseril, A.; Profeta, S., Jr.; Allinger, N. L. *J. Org. Chem.* **1987**, *52*, 5162.

(13) Goldsmith, D. J.; Bowen, J. P.; Qamhiyeh, E.; Still, W. C. *J. Org. Chem.* **1987**, *52*, 951.

(14) Lipkowitz, K. B.; Allinger, N. L. *QCPE Bulletin* **1987**, *7*, 19.

0002-7863/91/1513-4505$02.50/0